CHEMMEDCHEM

CHEMISTRY ENABLING DRUG DISCOVERY

Accepted Article

Title: Synthesis and Evaluation of In Vitro Biological Properties of Ferrocenyl Side-Chain-Decorated Paclitaxel

Authors: Damian Plażuk, Anna Wieczorek, Wojciech M. Ciszewski, Karolina Kowalczyk, Andrzej Błauż, Sylwia Pawlędzio, Anna Makal, Chatchakorn Eurtivong, Homayon J. Arabshahi, Jóhannes Reynisson, Christian G. Hartinger, and Błażej Rychlik

To be cited as: *ChemMedChem* 10.1002/cmdc.201700576

Link to VoR: http://dx.doi.org/10.1002/cmdc.201700576

A Journal of

ChemPubSoc Europe

WILEY-VCH

www.chemmedchem.org

WILEY-VCH

FULL PAPER

Synthesis and Evaluation of *In Vitro* Biological Properties of Ferrocenyl Side-Chain-Decorated Paclitaxel

Damian Plażuk[a]*, Anna Wieczorek[a], Wojciech M. Ciszewski[a], Karolina Kowalczyk[a], Andrzej Błauż[b], Sylwia Pawlędzio[c], Anna Makal[c], Chatchakorn Eurtivong[d], Homayon J. Arabshahi[d], Jóhannes Reynisson[d], Christian G. Hartinger[d], Błażej Rychlik[b]

Abstract: Taxanes, including paclitaxel, are widely used in cancer therapy. In an attempt to overcome some of the disadvantages entailed with taxane chemotherapy, we devised the synthesis of ferrocenyl-decorated paclitaxels and studied their biological properties. The cytotoxic activity was measured in a panel of human cancer cell lines of different tissue origin including also multidrug resistant ones. A structure-activity study of paclitaxel ferrocenylation revealed that the N-benzoyl ferrocenyl substituted derivative was the most cytotoxic. In contrast, substitution of the 3'-phenyl group of paclitaxel with a ferrocenyl moiety led to formation of relatively less potent antiproliferative agents. However, they were able to overcome multidrug resistance as they were virtually unrecognized by ABCB1, a major cellular exporter of taxanes. Interestingly, redox properties of ferrocenyl derivatives seemed to play a less important role in the mode of action of the investigated compounds as there was no correlation between intracellular redox activity and cytotoxicity/cell cycle distribution of cells. The antiproliferative activity of ferrocenyl taxanes strongly depended on the substitution position and good polymerisation inducers, as confirmed by molecular docking, were usually more cytotoxic, while compounds with stronger pro-oxidative properties exhibited lower antiproliferative activity.

[a] Prof. D. Plażuk, Dr. A. Wieczorek, Dr. W. M. Ciszewski, K. Kowalczyk
Department of Organic Chemistry
Faculty of Chemistry
University of Łódź
Tamka 12
91-403 Łódź (Poland)
E-mail: damplaz@uni.lodz.pl

[b] Dr. A. Błauż, Dr. B. Rychlik
Cytometry Lab
Department of Molecular Biophysics
Faculty of Biology and Environmental Protection
University of Łódź
Pomorska 141/143
90-236 Łódź (Poland)

[c] S. Pawlędzio, Dr. A. Makal
University of Warsaw
Biological and Chemical Research Centre
Żwirki i Wigury 101
02-096 Warsaw (Poland)

[d] C. Eurtivong, Dr. H. J. Arabshahi, Dr J. Reynisson, Prof. C. G. Hartinger
School of Chemical Sciences
Private Bag 92019
Auckland 1142 (New Zealand)

Supporting information for this article is given via a link at the end of the document.

Introduction

Antimitotic agents disrupt the mitotic progression of cells and thus they constitute an important class of drugs widely used in cancer therapy.[1] All registered antimitotic drugs interact with tubulin and either inhibit the polymerisation of α- and β-tubulin to microtubules or stabilise the microtubule structure thus preventing its depolymerisation back to tubulin. In both cases, a cell fails to assemble a functional mitotic spindle which results in its death.[1] Taxanes, such as paclitaxel **1** (Figure 1), belong to the group of antimitotic agents. Paclitaxel promotes polymerisation of tubulin, stabilises microtubules and impairs their dynamics, leading to a mitotic arrest and induction of apoptosis of cancer cells.[2] It is widely used in therapy of breast and ovarian carcinomas as well as Kaposi's sarcoma, however, the usage of taxanes in anticancer therapy results in numerous adverse effects.[3]
Additionally, in some cases, taxanes are not sufficiently effective in cancer therapy due to the development of the multidrug-resistance (MDR). There are several mechanisms of paclitaxel resistance but one of the most important is attributed to elevated activity of ATP-binding cassette transporters such as ABCB1 (also known as P-glycoprotein, P-gp) or multidrug-resistance associated-protein (MRP, also known as ABCC1), which are responsible for the efflux of xenobiotics from a cell.[4] The high activity of ABCB1 significantly decreases the intracellular concentration of the anticancer agent leading to a therapy failure. Thus, it is highly desirable to develop novel antimitotic agents, which are able to overcome MDR and are more effective toward taxane-resistant tumours.
The conjugation of biologically active compounds with organometallic moieties, such as ferrocene, emerged as a promising strategy.[5] In the last two decades, a large number of ferrocenyl conjugates with biologically important vectors were synthesised and their anticancer,[6] antimalarial,[7] and antimicrobial[8] activities were investigated. In many cases this approach resulted in compounds of significantly enhanced activity when compared to their organic counterparts. Moreover, incorporation of a ferrocenyl moiety into an organic drug may significantly change its mode of action. For example, a ferrocenyl amino acid derivative demonstrated anticancer activity towards MDR cancer cells,[9] or a ferrocenyl-substituted tamoxifen

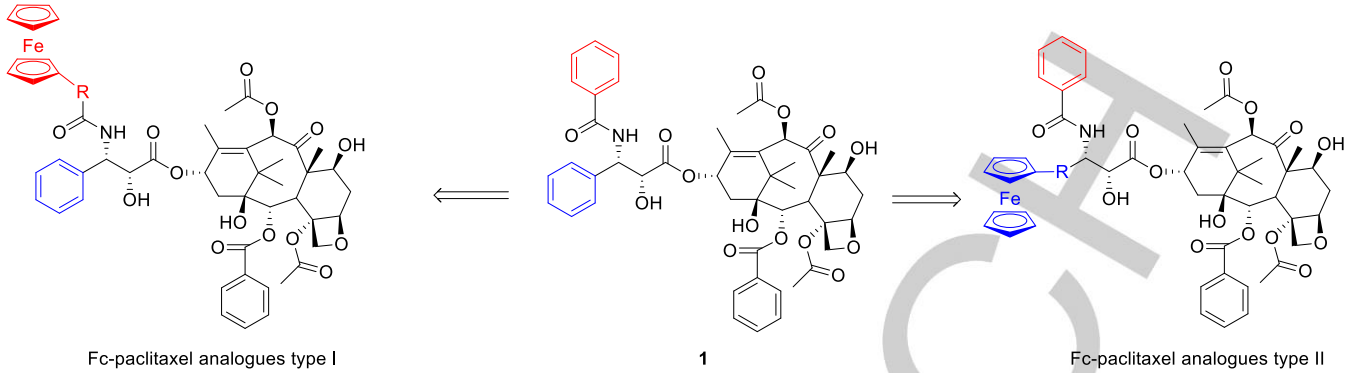

Figure 1. General structures of paclitaxel **1** and its ferrocenyl analogues type I and II

derivative benefitted from the redox properties of ferrocene.[10] Similarly, a ferrocenyl analogue of the antimalarial drug chloroquine, i.e. ferroquine, was able to overcome drug resistance of *Plasmodium*.[11] We demonstrated that a ferrocenyl analogue of plinabulin was an inhibitor of ABCB1 and ABCG2 and was even more cytotoxic towards MDR cancer cells against which plinabulin itself was not active.[12] The positive impact of the ferrocenyl moiety on the anticancer or antimalarial activity of ferrocenyl drug conjugates is often attributed to the redox properties of the metallocene moiety and its ability to generate reactive oxygen species (ROS). ROS are able to modify DNA and other important biological molecules leading to cell death.[5a, 13]

We have previously reported that the incorporation of a ferrocenyol moiety instead of an *N*-benzoyl group in a side-chain of paclitaxel significantly increased its cytotoxicity and ability to induce tubulin polymerisation and, consequently, apoptosis.[14] Based on these promising results, the influence of the ferrocenyl moiety on the biological properties of paclitaxel was studied here in detail. We report the synthesis of two series of ferrocenyl analogues of paclitaxel (the generic structure of both are depicted in Figure 1), and their biological properties, in particular cytotoxicity, cell cycle effects, ROS generation, ability to induce tubulin polymerisation, and docking to tubulin.

Results and Discussion

Synthesis

Type I ferrocenyl analogues of paclitaxel (Figure 1) were synthesised following an established literature method, which was developed for the synthesis of N-debenzoyl-N-ferrocenoylpaclitaxel.[14] First, (*3R,4S*)-3-triethylsilyloxy-4-phenylazetidin-2-one was *N*-acylated in a reaction with ferrocenoyl and *o*-, *m*-, and *p*-ferrocenylbenzoyl chloride which was freshly synthesised in a reaction of the corresponding

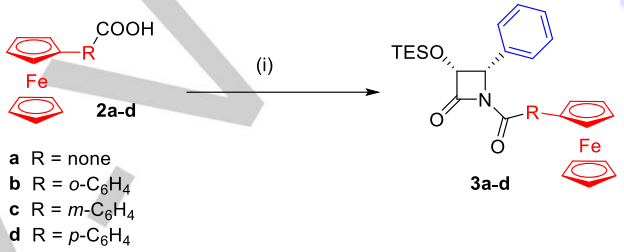

Scheme 1. Synthesis of *N*-substituted azetidin-2-ones **3a-d**. Reagents and conditions: (i) $(COCl)_2$, DMF, DCM, RT, 2h; then (*3R,4S*)-3-triethylsilyloxy-4-phenylazetidin-2-one, TEA, DMAP, DCM, RT, 0°C

acids **2a-d** with oxalyl chloride (Scheme 1). Then, the *N*-substituted azetidin-2-ones **3a-d** were reacted with **4** in the presence of LiHMDS at -40 °C for 40 min and gave **5a-d** in good yields. Deprotection of the 2'- and 7-OH groups in **5a-d** with HF·Py was carried out in acetonitrile-pyridine solution at RT for 24 h. This led to the desired **N**- ferrocene-substituted paclitaxels **6a-d** in good to excellent yields (Scheme 2). In order to synthesise type II ferrocenyl analogues of paclitaxel, access to optically pure (*3R,4S*)-3-hydroxy-4-ferrocenylazetidin-2-ones **9a-d** was required and they were synthesised in multistep reactions. First, in a reaction of trimethylsilyl trimethylsilyloxyacete **7** with an excess of LiHMDS and TMSCl a solution of 1,1,2-trimethoxyethene was generated, followed by reaction with freshly prepared N-TMS-imines (formed in situ from ferrocenecarboxaldehyde or *o*-, *m*-, or *p*-ferrocenylbenzaldehyde and an excess of LiHMDS) and an excess of TMSCl to give the corresponding *cis*-4-ferrocene-substituted azetidin-2-ones **8a-d** as the major isomers. Because these compounds were not stable (only **8a** was isolated in a pure form), the trimethylsilyl groups were removed in a reaction with an excess of TBAF in THF. Pure *cis*-**9b-d** were isolated in good overall yields (Scheme 3).

As **9a** was not stable, the OH group in **9a** was protected in a reaction with TESCl in pyridine to give stable **10a**. (*3S,4R*)- and (*3R,4S*)-enantiomers of the **10a** and **10b-c** were separated by preparative chiral HPLC. Compound **9d** required *O*-triethylsilylation to **10d** prior to preparative separation of the enantiomers on a chiral HPLC column. In all cases, the

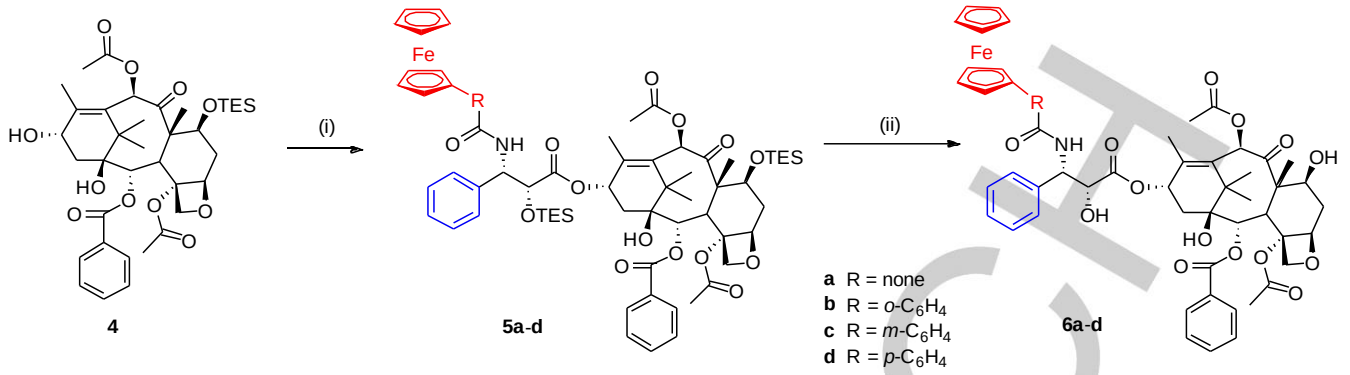

Scheme 2. Synthesis of the *N*-ferrocenyl-decorated paclitaxels **5a-d** and **6a-d**. Reagents and conditions: (i) **3a-d**, LiHMDS, THF, -40°C, 50 min; (ii) HF·Py, MeCN, Py, RT, 24h

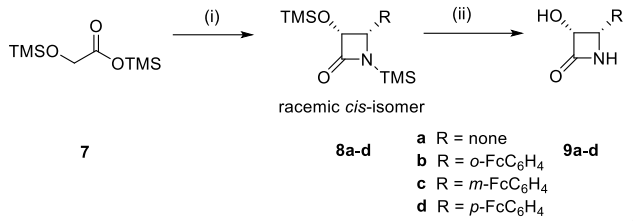

Scheme 3. Synthesis of the 4-ferrocenyl- and 4-(ferrocenylphenyl)-3-hydroxyazetidin-2-ones **9a-d**. Reagents and conditions: (a) LiHMDS, THF, TMSCl 0°C, then RCHO, 0°C, then TMSCl, RT 24h; (b) TBAF, THF, RT

(*3S,4R*)-enantiomers were eluted as the 1st fraction while (*3R,4S*)-enantiomers were collected as the 2nd fraction. Absolute configurations of the ferrocenyl azetidin-2-ones were confirmed by X-ray crystallography (see SI). In the next step (*3S,4R*)- and (*3R,4S*)-**10a-d** were converted with benzoyl chloride in pyridine and DMAP in DCM into the *N*-benzoyl derivatives (*3S,4R*)- and (*3R,4S*)-**11a-d**, respectively (Scheme 4). Finally, (*3R,4S*)-**11a-d** were reacted with **4** in the presence of LiHMDS at -40° C for 40 min to give **12a-d**, while the reaction of (*3S,4R*)-**11a-e** with **4** provided **14a-d**. The deprotection of the 2'- and 7-OH groups in **12a-d** and **14a-d** in a reaction with HF·Py resulted in the desired ferrocenyl analogues of paclitaxel (**13a-d**) and 2',3'-epi-paclitaxel (**15a-d**; Scheme 5).

Antiproliferative activity in human cancer cells

The antiproliferative potency of the synthesised compounds was investigated in the human tumour cell lines A549 (alveolar basal epithelial cell adenocarcinoma), Colo 205 (colorectal adenocarcinoma), HCT116 (colorectal adenocarcinoma), Hep G2 (hepatocellular carcinoma), MCF7 (breast adenocarcinoma) and SW620 (colorectal adenocarcinoma). Additionally, we employed a panel of five multidrug resistant cell lines derived from SW620 and characterised by overexpression of various ABC proteins, namely ABCG2 (SW620C line), ABCC1 (SW620M and SW620E lines) and ABCB1 (SW620D, SW620E, and SW620V lines).[15]

The ferrocenyl 2',3'-epi-paclitaxel derivatives **15a-d** were virtually not active towards any cell line in the concentration range studied with a notable exception of **15a**, to which SW620 Colo 205 and MCF7 were susceptible (Table 1). Even then, however, the cytotoxicity of the ferrocenyl 3'-substituted compound was 2–3 times lower than that of the parent compound 2',3'-epi-paclitaxel. In contrast, all of the synthesised ferrocenyl analogues of paclitaxel exhibited cytotoxic activity in the nM or μM concentration range. Their activity strongly depended on the position of the ferrocenyl moiety attached to the side-chain of paclitaxel. In general, the *N*-benzoyl substituted compounds were the most active against all the cell lines studied. This indicates the impact of a single substitution of the *N*-benzoyl group with a ferrocenoyl moiety, as earlier demonstrated in other cases.[14] Additionally, it became apparent that the spatial positioning of the ferrocenyl group at the side chain of paclitaxel impacts the biological properties as m-substituted **6c** was more active than p-substituted **6d**. Notably, o-substituted **6b** was even an order of magnitude less active in the cell lines studied. On the other hand, replacement of the 3'-phenyl moiety of the phenylisoserine side-chain of paclitaxel with a ferrocenyl group (**13a**) decreased the cytotoxic activity of the corresponding conjugate by roughly two orders of magnitude compared to both paclitaxel and **6a**. The cytotoxicity of the compounds bearing ferrocenyl-decorated phenyl groups **13b-d** was again generally lower than the simple compound **13a**. However, in this case the activity of o- and m-substituted **13b** and **13c** was higher than of *p*-substituted **13d**. No correlation between tissue origin of a cell line and toxicity pattern could be found, although A549 was usually the least chemo-responsive cell line followed by HCT116 and Hep G2.

Table 1. Cytotoxicity of the ferrocenyl taxanes **6a-d**, **13a-d** and **15a-d** in comparison to paclitaxel **1** and 2',3'-epi-paclitaxel as determined by neutral red uptake assay.[a]

	IC_{50} [μM]					
	SW620	A549	Colo 205	HCT116	Hep G2	MCF7
6a	0.009 [0.007-0.010]	0.015 [0.010-0.023]	< 0.005	< 0.005	< 0.005	< 0.005
6b	1.118 [0.546-3.552]	1.605 [0.106-24.40]	0.877 [0.444-1.732]	8.147 [2.216-29.95]	1.675 [0.951-2.948]	0.734 [0.104-5.202]
6c	0.122 [0.107-0.139]	0.100 [0.082-0.121]	0.072 [0.057-0.090]	0.072 [0.064-0.082]	0.105 [0.042-0.260]	0.053 [0.041-0.070]
6d	0.229 [0.132-0.397]	0.128 [0.061-0.273]	0.202 [0.112-0.363]	0.206 [0.061-0.700]	0.103 [0.076-0.139]	0.129 [0.055-0.302]
13a	0.490 [0.366-0.655]	1.299 [0.531-3.176]	0.286 [0.221-0.370]	0.506 [0.324-0.790]	0.793 [0.395-1.590]	0.377 [0.263-0.540]
13b	1.976 [1.442-2.708]	>50	2.811 [2.330-3.392]	>50	3.475 [2.247-5.374]	1.203 [0.875-1.652]
13c	2.441 [1.429-4.169]	10.22 [1.663-62.79]	7.497 [1.097-51.22]	27.88 [3.281-236.8]	1.457 [0.637-3.330]	1.209 [0.507-2.883]
13d	2.103 [1.245-3.552]	>50	>50	>50	>50	0.747 [0.500-1.115]
15a	0.926 [0.283-3.025]	>50	1.995 [0.377-10.56]	>50	>50	1.056 [0.732-1.524]
15b	1.437 [0.263-7.835]	>50	>50	>50	>50	>50
15c	>50	>50	>50	>50	>50	>50
15d	>50	>50	>50	>50	>50	>50
1	0.015 [0.011-0.020]	0.005 [0.004-0.006]	< 0.005	< 0.005	< 0.005	< 0.005
2',3'-epi-paclitaxel	1.924 [1.450-2.552]	1.071 [0.549-2.090]	0.668 [0.309-1.443]	0.379 [0.292-0.491]	0.395 [0.105-1.484]	0.452 [0.329-0.620]

[a] 95%-confidence intervals are given in brackets (please note that due to the log-transformation of the data required to perform IC_{50} calculations, these are asymmetrical). The IC_{50} values were calculated based on three independent experiments. >50 denotes situations in which the IC_{50} values were not possible to determine (<50% viability was not achieved in the concentration range used (5 nM - 50 μM)). < 0.005 denotes situations in which the calculated IC_{50} values were below the lowest concentration used.

The anticancer activity of taxanes is dependent on the level of expression of the efflux protein ABCB1 in cancer cells.[16] In order to elucidate the impact of ferrocene substitution on the mode of action of these, the cytotoxicity of the newly synthesised compounds was determined in an SW620-based multidrug resistant cell line panel with the neutral red assay based on lysosomal integrity of viable cells (Table 2). Independently of the compound studied, the susceptibility of SW620C and SW620M cells was comparable to that of the parental SW620 cells. This is not surprising as none of these cell lines express active ABCB1.[15] On the other hand, ABCB1-expressing SW620D, SW620E and SW620V cells were significantly more resistant towards paclitaxel and its ferrocene derivatives. The level of resistance, expressed as the ratio of the maximal of IC_{50} values against SW620D, SW620E or SW620V cells to the IC_{50} value in SW620 cells for a given substance, was the highest for **6a** and paclitaxel (41 and 54, respectively) and the lowest for **13b** and **13c** (1.6 and 1.5, respectively). The sensitization potential of **13b** and **13c** could be important for the design of taxane derivatives able to overcome the multidrug resistance of cancer cells. It should be emphasized here that we attempted also to assess direct interactions between investigated taxol derivatives and ABCB1 protein in an indirect transport assay (direct measurement of radiolabeled taxol transport via the cellular membrane is impossible due to high lipophilicity of this substance). However, we failed despite using a range of different recognized substrates of ABCB1 (calcein AM, rhodamine 123 and

Table 2. Cytotoxicity of the ferrocenyl taxanes **6a-d**, **13a-d** and **15a-d** in comparison to **1** and 2',3'-epi-paclitaxel as determined by neutral red uptake assay.[a]

	IC_{50} [μM]					
	SW620	SW620C	SW620D	SW620E	SW620M	SW620V
6a	0.009 [0.007-0.010]	0.008 [0.006-0.013]	0.274 [0.090-0.836]	0.254 [0.121-0.537]	0.007 [0.005-0.010]	0.366 [0.249-0.537]
6b	1.118 [0.546-3.552]	0.642 [0.194-2.125]	4.663 [3.282-6.626]	2.300 [1.035-5.111]	0.646 [0.343-1.214]	3.002 [2.31-3.93]
6c	0.122 [0.107-0.139]	0.108 [0.085-0.136]	1.584 [0.419-5.997]	1.560 [0.335-7.269]	0.124 [0.107-0.143]	1.557 [0.719-3.37
6d	0.229 [0.132-0.397]	0.192 [0.090-0.409]	2.738 [0.179-41.85]	1.894 [0.715-5.019]	0.226 [0.117-0.436]	2.771 [1.098-6.99
13a	0.490 [0.366-0.655]	0.365 [0.274-0.486]	2.115 [1.653-2.706]	2.007 [1.683-2.392]	0.525 [0.403-0.684]	1.939 [1.570-2.39
13b	1.976 [1.442-2.708]	1.825 [1.080-3.082]	4.174 [2.486-7.009]	4.247 [2.842-6.347]	2.292 [1.932-2.719]	3.174 [2.551-3.94
13c	2.441 [1.429-4.169]	2.771 [1.301-5.899]	4.874 [1.590-14.94]	3.687 [1.347-10.09]	4.917 [2.256-10.71]	6.757 [1.138-40.1
13d	2.103 [1.245-3.552]	1.998 [0.869-4.594]	>50	>50	3.512 [1.218-10.13]	>50
15a	0.926 [0.283-3.025]	1.235 [0.055-27.80]	>50	>50	0.915 [0.386-2.169]	>50
15b	1.437 [0.263-7.835]	2.397 [0.143-40.16]	>50	>50	>50	>50
15c	>50	>50	>50	>50	>50	>50
15d	>50	>50	>50	>50	>50	>50
1	0.015 [0.011-0.020]	0.011 [0.008-0.016]	0.810 [0.335-1.960]	0.519 [0.336-0.801]	0.011 [0.008-0.015]	0.566 [0.420-0.76
2',3'-epi-paclitaxel	1.924 [1.450-2.552]	0.875 [0.054-14.29]	40.36 [2.453-664]	8.417 [4.434-15.98]	1.446 [1.162-1.800]	23.29 [2.687-202

[a] 95%-confidence intervals are given in brackets (please note that due to the log-transformation of the data required to perform IC_{50} calculations, thes asymmetrical). IC_{50} values were calculated based on three independent experiments. >50 denotes situations in which the IC_{50} values were not possible to dete (<50% viability was not achieved in the concentration range used (5 nM - 50 μM)). < 0.005 denotes situations in which the calculated IC_{50} values were below the limit of concentration range

doxorubicin). Astonishingly, we found only one successful literature report[17] demonstrating interactions between paclitaxel and ABCB1 by calcein AM and rhodamine 123 uptake assays but we considered the experimental conditions used by the Authors (very high concentrations of dyes and taxol and long incubation periods) rather harsh.

Interaction with tubulin

The main mechanism of taxane cytotoxic activity is based on their ability to induce tubulin polymerisation and to stabilise microtubules. Preliminary studies showed that introduction of a ferrocenyl moiety into the side-chain of paclitaxel increases the ability of selected compounds to induce polymerisation of tubulin. Driven by this observation, we studied the ability of the synthesised compounds to induce polymerisation of tubulin. Only compounds namely **6a**, **6c**, **13a** and 2',3'-epipaclitaxel (Figures 2, S1 and S2) were able to induce tubulin polymerisation at least as efficiently as paclitaxel. All other compounds were much weaker polymerisation promotors unable to induce tubulin polymerisation even at high concentrations. Earlier studies suggested that the higher cytotoxic activity of compound **6a** compared to **1** is based on its higher potency to promote tubulin polymerisation.[14]

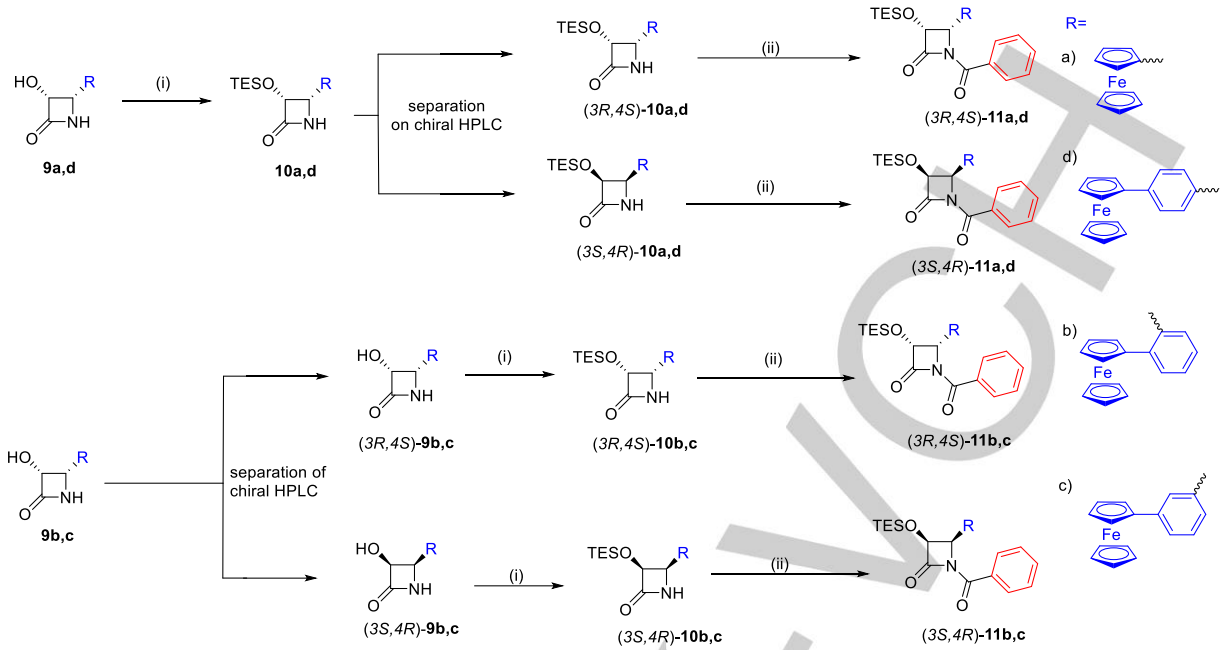

Scheme 4. Synthesis of the (*3R,4S*)- and (*3S,4R*)-4-ferrocenyl- and 4-(ferrocenylphenyl)-*N*-benzoyl-3-hydroxyazetidin-2-ones **11a-d**. Reagents and conditions: (i) TESCl, PyH, RT, 50 min; (ii) PhCOCl, TEA, DMAP, DCM, RT, 2h

However, in the series of compounds reported herein, there is no clear correlation between their antiproliferative activity and the ability to induce tubulin polymerisation. For example, compound **6c** is more cytotoxic than **13a** against the cells studied but exhibits lower potency as a tubulin polymerisation promoter, even at high concentrations of 30 µM.

Cell cycle impairment

The influence of ferrocenyl analogues of paclitaxel on the cell cycle was investigated in SW620 and SW620V cancer cells after incubation of the cells with 10 nM of the ferrocenylcompounds for 48 h. Only paclitaxel and **6a** significantly affected the cell cycle in SW620 cells, while no changes were observed for all other compounds (Figures S3 and S4). These results may suggest that mitotic arrest plays only a limited role in the antiproliferative activity of the ferrocenyl taxanes with the notable exception of **6a** (see Fig. S3). One should bear in mind, however, that we employed a very low concentration in this experiment and more detrimental, although artefactual, effects might be observed at higher doses of the investigated compounds.

Generation of reactive oxygen species

Paclitaxel is able to generate reactive oxygen species but the mechanism of ROS formation and its therapeutic implications are still not fully understood.[18] Ferrocene is redox active and the mechanism of biological activity of ferrocenyl

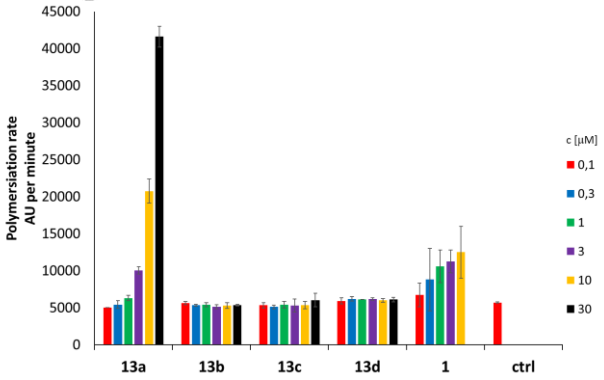

Figure 2. Concentration-dependent ability to induce tubulin polymerisation by compounds **13a-d** in comparison to **1**. Data for compounds **6a-d** and **15a-d** are shown in Figure S1 and Figure S2

compounds were suggested to involve redox processes at the ferrocenyl moiety. Thus, the ability of ferrocenyl taxanes to generate ROS was determined in SW620 cells (Figure 3). ROS formation was measured by dihydrorhodamine 123 oxidation and was found to be strongly dependent on the location of the ferrocenyl substituent in the side-chain of paclitaxel. Compound **13a** bearing a ferrocenyl moiety instead of a 3'-phenyl group exhibited much higher pro-oxidative potency than its counterparts featuring a ferrocenyl group in *o*-, *m*- or *p*-position to the 3'-phenyl moiety. Moreover, the cytotoxic

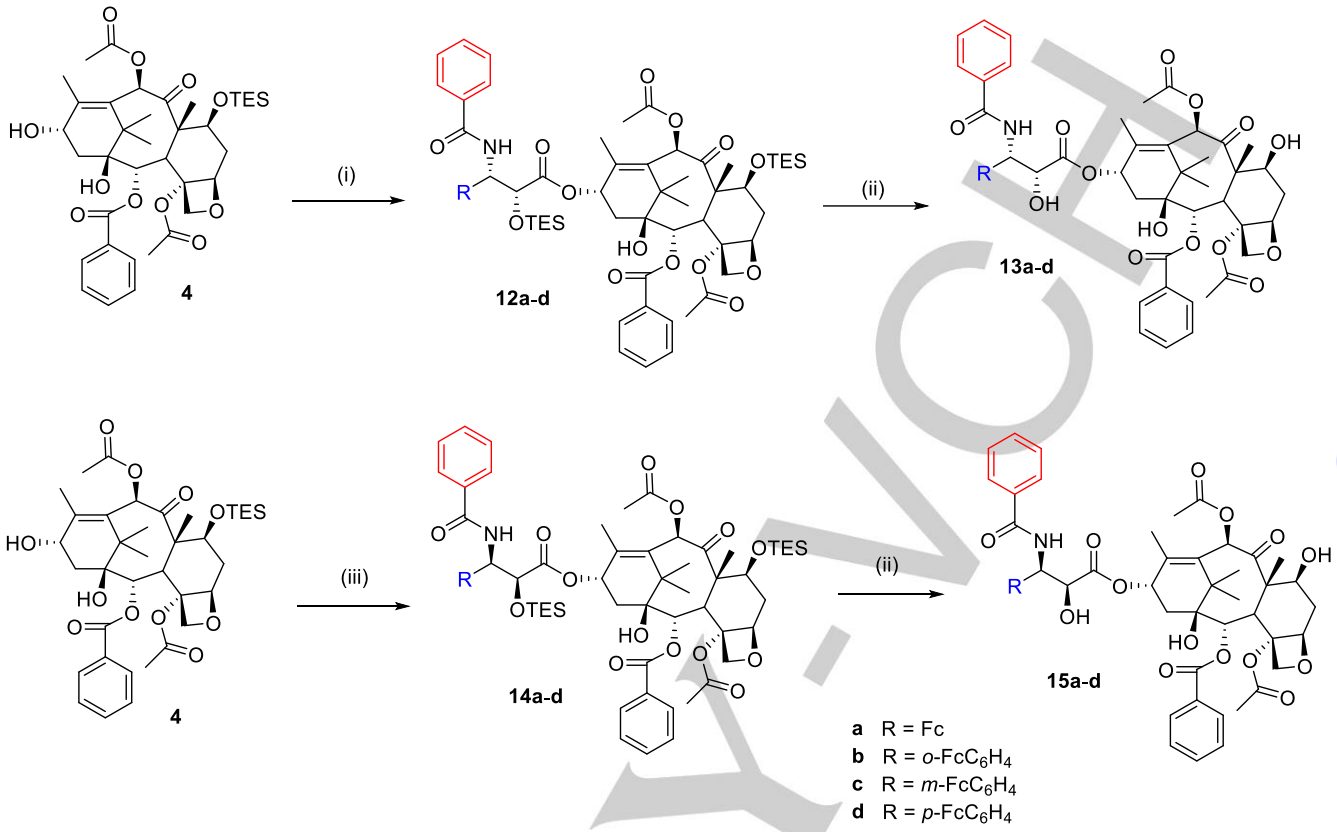

Scheme 5. Synthesis of the 3'-dephenyl-3'-ferrocenyl and 3'-(ferrocenylphenyl)paclitaxel derivatives **13a-d** and the 2',3'-epi-paclitaxel derivatives **15a-d**. Reagents and conditions: (i) (*3R,4S*)-**11a-d**, LiHMDS, THF, -40ºC, 50 min; (ii) HF·Py, PyH, MeCN, RT, 24h; (iii) (*3S,4R*)-**11a-d**, LiHMDS, THF, -40ºC

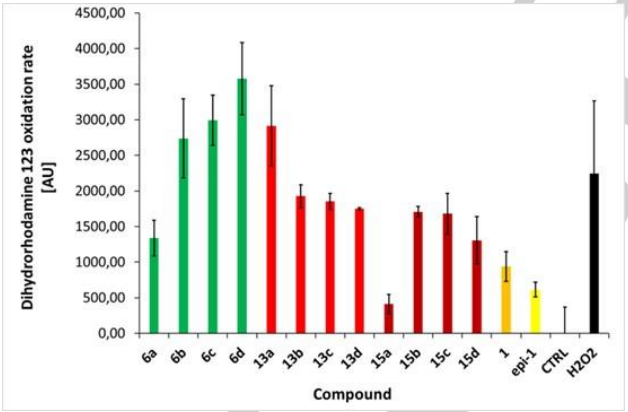

Figure 3. Reactive oxygen species formation in SW620 cells induced by ferrocenyl taxanes and compared to paclitaxel **1** and 2'3'-epi-paclitaxel epi-1 as well as H_2O_2 as a positive control

activity of this series of compounds corresponded to their ability to generate ROS. In contrast, there was no correlation between the ROS generation ability and cytotoxic activity in compounds **6a-d** bearing a ferrocenyl moiety instead of the 3'-*N*-phenyl group. The most cytotoxic **6a** is less pro-oxidative than **6b-d**, which effectively generate ROS but are less toxic. With the exception of **15a**, epi-derivatives induce ROS more effectively than paclitaxel but they are much less cytotoxic. Summarising, almost all ferrocenyl compounds studied are more potent in terms of ROS generation than paclitaxel but there is no clear correlation between their pro-oxidative potency and cytotoxicity. These results suggest that ROS generation plays a minor role in the mechanism of cytotoxic activity of ferrocenyl taxanes.

Docking of ferrocenyl paclitaxel derivatives to tubulin

Despite numerous attempts to obtain crystals of tubulin complexed with ferrocenyl taxanes, we were unfortunately unable to obtain crystals suitable for X-ray analysis. Thus, to explain the influence of a ferrocenyl moiety on the interaction of paclitaxel with tubulin, molecular docking was employed to investigate the possible binding mode for a series of ferrocenyl paclitaxel derivatives to tubulin. The tubulin crystal structure co-crystallised with paclitaxel was obtained from the Protein Data Bank (PDB ID: 1JFF). Paclitaxel was removed from the tubulin structure and re-docked with excellent docking overlays (RMSD = 1.43 Å). In addition, the binding modes obtained were

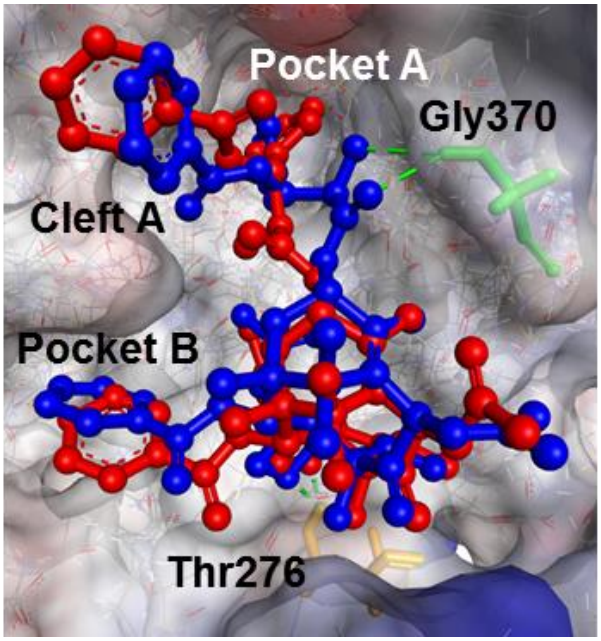

Figure 4. Configuration of the co-crystallised ligands paclitaxel (blue) and 2',3'-epi-paclitaxel (red). Hydrogen bonds are represented as green dotted lines between paclitaxel and the residues Gly370 and Thr276 coloured green and orange. The protein surface is rendered where grey, red and blue areas depict neutral, positively and negatively partial-charged regions, respectively

similar to those reported in literature,[19] justifying the reliability and reproducibility of the docking protocol. Hydrogen bonding was observed with Gly370 and Thr276. The ferrocenyl paclitaxel derivatives and epi-paclitaxel were docked to the taxol site using the GoldScore (GS) function to determine the predicted binding modes and affinities represented by score values (Table S5). The best predicted binding mode and hydrogen bond interactions of epi-paclitaxel (Figure 4) closely resembled the co-crystallised paclitaxel ligand and the scores of the derivatives were relatively similar to their counterparts paclitaxel and 2',3'-epi-paclitaxel. Rendering of the protein surfaces showed that the majority of the area of the taxol binding site is hydrophobic (Figure 4) and is occupied mainly by the diterpene core and the phenyl rings. The diterpene core sat above a hydrophobic basin composed of Pro274, Leu275, and backbones of Arg278, Ser277 and Gln282. Additionally, the diterpene core was found in close proximity to hydrophobic amino acids such as a leucine cluster consisting of Leu286, Leu371 and Leu375 which can form lipophilic contacts with the ligand. The C3' benzamido group occupied the hydrophobic cleft A situated above His229 whereas the phenyl at C3' lied within the hydrophobic pocket accommodated by the residues Pro360, Thr240, Val23, Ala233, and Phe272. The lipophilic pocket B was naturally occupied by the C2 benzoyl ring and was formed mainly by Ile212 and a cluster of leucine residues (Leu209, Leu217, Leu227, Leu230 and Leu275). Negligible changes in binding modes and interactions were seen for

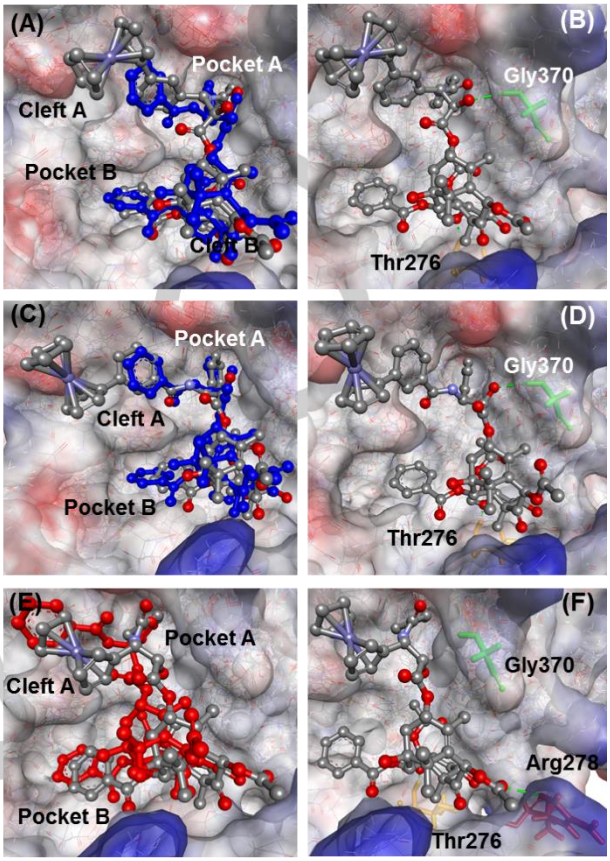

Figure 5. Docked configurations of **13c** (A), **6c** (C), and **15a** (E) and their corresponding hydrogen bonding is shown in B, D and F. The derivatives are overlaid with the co-crystallised ligands paclitaxel (blue) and epi-paclitaxel (red). Hydrogen bonds are depicted as green dotted lines, and the involved amino acid residues are coloured and labelled; Gly370 green, Arg278 red and Thr276 orange. The protein surface is rendered red (negatively charged), blue (positively charged) and grey (neutral) which represent neutral, negatively and positively partial charged regions, respectively.

ferrocenyl substitutions as represented by the *m*-ferrocenyl substituted derivatives **13c** and **6c** (Figures 5A and 5C). The C3' phenyl and benzamido rings as well as the C2' benzoyl group retained their occupation in the respective binding pockets and clefts as observed for paclitaxel (blue) and epi-paclitaxel (red). Additionally, the oxetane ring and the C2'-hydroxy residue maintained their interactions with Thr276 and Gly370. On the other hand, the 2',3'-epi-paclitaxel derivatives exemplified by **15a** varied slightly in pose (Figure 5E). Notably, a change in stereochemistry at C2' and C3'distorted the benzamido ring from cleft A. Occasionally, the benzamido ring was seen to occupy pocket A, whereas the ferrocenyl substituted phenyl occupied cleft A as in the case of **15c** and **15d**.

Conclusions

Two series of ferrocenyl analogues of paclitaxel were synthesised and their biological properties were evaluated. The cytotoxic activity of the compounds was studied towards a panel of human cancer cell lines of different tissue origin and it was found strongly dependent on the position of the ferrocenyl group, with the *N*-benzoyl substituted compounds **6a-d** being the most active derivatives. We demonstrated also that the mechanism of ferrocenyl taxane antiproliferative activity varied depending on the structure and that good polymerisation inducers, as also confirmed by molecular docking, are usually more cytotoxic, while compounds with stronger pro-oxidative properties exhibited lower antiproliferative activity. The results obtained, however, suggest that there is no universal mechanism of ferrocenyl taxane mode of action as some significantly cytotoxic compounds poorly interacted with tubulin. The effects observed await more elaborated explanation. Interestingly, the substitution of a 3'-phenyl group with a ferrocenyl moiety (**13b** and **13c**) leads to relatively low toxicity compounds that are however able to overcome multidrug resistance as they are virtually unrecognized by ABCB1, which is a major cellular exporter of taxanes. This could be a new lead for the discovery of anticancer agents based on the taxane structure able to overcome resistance.

Experimental Section

Synthesis

All reactions were conducted using standard Schlenk techniques under argon atmosphere. Chemicals and solvents (HPLC grade) were purchased from Sigma-Aldrich and used as received. Compound **6a** was synthesised as described previously.[14] 1D (^{1}H, ^{13}C{^{1}H} and ^{13}C DEPT 135) and 2D (^{1}H-^{1}H COSY, ^{1}H-^{13}C HSQC, ^{1}H-^{13}C HMBC) NMR spectra were recorded on a Bruker ARX 600 MHz (spectrometer frequency 600.3 MHz for ^{1}H and 150.9 MHz for ^{13}C). Chemical shifts for the ^{1}H NMR spectra are referenced relative to residual protons in the deuterated solvent ($CDCl_3$ δ = 7.26 ppm for ^{1}H and δ = 77.00 ppm for ^{13}C{^{1}H}; DMSO-d_6 δ = 2.50 ppm for ^{1}H and δ = 39.51 ppm for ^{13}C{^{1}H}; C_6D_6 δ = 7.16 ppm for ^{1}H and δ = 128.6 ppm for ^{13}C{^{1}H}). Spectra were recorded at room temperature (291 K), chemical shifts are in ppm and coupling constants in Hz. Electrospray MS (ESI-MS) spectra were recorded on a Varian 500-MS spectrometer at 50 V (compounds were dissolved in methanol). Optical rotation $[a]_D^{20}$ was measured at room temperature (293 K) using 241 MC (Perkin-Elmer) or MCP 500 (Anton Paar) polarimeter. Thin-layer chromatography (TLC) was performed on aluminium sheets precoated with Merck 5735 Kieselgel 60 F254. Column chromatography was conducted with FLUKA 60752 Silica gel 60 for flash chromatography (0.040-0.063 mm 230-400 mesh). The purity of all the compounds studied in biological assays was higher than 95% as demonstrated by HPLC. HPLC analyses were performed with Shimadzu Prominence system equipped with a PDA detector and using a Phenomenex Kinetex 5µ PFP 100 Å column 150 × 4.6 mm. A gradient was applied using eluents A (0.1% TFA in acetonitrile) and B (0.1% TFA in water), starting from A:B = 30:70 to A:B = 90:10 within 20 min, then A:B =90:10 for 10 min, and A:B = 30:70 for 10 min. Detection was accomplished at λ = 220 nm and 254 nm and a flow rate of 1 mL/min was used. Preparative HPLC were performed as described below.

(*3R,4S*)-*N*-(2-ferrocenylbenzoyl)-3-triethylsilyloxy-4-phenylazetidin-2-one (**3b**) was prepared in 67% yield (640 mg) following a literature procedure[14] starting from 800 mg (2.6 mmol) of 2-ferrocenylbenzoic acid (**2b**), 1.05 g (8.28 mmol) of oxalyl chloride, 470 mg (1.69 mmol) of (*3R,4S*)-3-triethylsilyloxy-4-phenylazetidin-2-one and 607 mg (6.0 mmol) of triethylamine. The crude product was purified on silica using n-hexane/ethyl acetate (4:1). Due to low stability it was used immediately in the next step.

(*3R,4S*)-N-(3-ferrocenylbenzoyl)-3-triethylsilyloxy-4-phenylazetidin-2-one (**3c**) was prepared in 23% yield (224 mg) according to the synthesis of **3b** starting from 800 mg (2.02 mmol) of 3-ferrocenylbenzoic acid (**2c**) instead of **2b**. Due to low stability it was used immediately in the next step.

(*3R,4S*)-*N*-(4-ferrocenylbenzoyl)-3-triethylsilyloxy-4-phenylazetidin-2-one (**3d**) was prepared in 42% yield (409 mg) according to the synthesis of **3b** starting from 800 mg (2.6 mmol) of 4-ferrocenylbenzoic acid (**2d**) instead of **2b**. Due to low stability it was used immediately in the next step.

General procedure A – Synthesis of azetidinones 8a-d

***cis*-4-ferrocenyl-3-trimethylsilyloxy-1-trimethylsilylazetidin-2-one** (**8a**) was prepared in slightly modified known procedure of synthesis of 3-hydroxy-4-phenylazetidin-2-one.[20] A solution of hexamethyldisilazane (HMDS) (7.81 g, 10.14 mL, 48.4 mmol) in 10 ml of anhydrous 1,2-dimethoxyethane was cooled to 0 °C and 26.3 mL of n-butyllithium (n-BuLi) (1.6 M, 42.0 mmol) was added. After 5 min of stirring, a mixture of 4.85 g (5.37 mL, 22.0 mmol) of trimethylsilyl trimethylsiloxyacetate and 2.39 g (2.81 mL, 22.0 mmol) of chlorotrimethylsilane (TMSCl) was added over 5 min to the freshly generated solution of LiHMDS. After 5 min of stirring a solution of 4.28 g (20.0 mmol) ferrocenecarboxaldehyde in 15 mL of 1,2-dimethoxyethane was added over 15 min at 0 °C. The resulting solution was stirred at RT for another 15 h and 2.16 g of chlorotrimethylsilane (2.64 mL, 20.0 mmol) was added. After 5 min, 120 mg of acetic acid (AcOH) and 0.50 g of triethylamine (TEA) were added. The solution was diluted with 30 ml of n-hexane and the mixture was filtered through a Celite pad. The organic phase was evaporated to dryness and the product was dissolved in hot n-heptane while insoluble material was filtered off. After evaporation of the solvents, the crude product was used in the next step without further purification. The pure product was obtained by crystallization. A solution of the product in n-heptane was evaporated to a small volume (ca. 50 mL) and was stored in a fridge at -24 °C for 24 h. Large orange crystals formed which were collected by filtration, washed with cold n-pentane (-40 °C) and dried under vacuum. The mother liquor was concentrated and stored in the fridge for another 24 h. Pure product (2.123g, 5.11 mmol, 26% yield) was obtained as orange crystals which were immediately used in the next step.

***cis*-4-ferrocenyl-3-hydroxyazetidin-2-one** (**9a**): 12g (45.9 mmola) of TBAF·3H_2O was added to a solution of crude **2a** in 60 mL of tetrahydrofurane and the resulting solution was stirred at RT for 2 h. 100 mL of water was added and the product was extracted with ethyl acetate. The organic phase was washed with brine, dried over sodium sulphate and evaporated to dryness. 50 mL of ethyl acetate was added to the crude product and the product was collected by filtration, washed with ethyl acetate (50 mL), n-pentane (100 mL), diethyl ether (100 mL) and dried. The crude product was obtained in 46% overall yield (2.50

g) as a yellow powder. As this compound is not very stable, it was immediately in the next step.

General procedure B – Synthesis of azetidinones 9b-d

***cis*-4-(2-ferrocenylphenyl)-3-hydroxyazetidin-2-one** (**9b**): 4.0 g (15.3 mmol) of TBAF·3H_2O was added to a solution of crude **8d** in 20 ml of THF, and the resulting solution was stirred for 80 min at RT. After addition of 100 mL of *tert*-butyl methyl ether and 50 mL of water, the product was extracted with ethyl acetate. Chromatography on silica gel (150 mL) using n-hexane/ethyl acetate (1:2), followed by dichloromethane/ethyl acetate (1:1) gave 1.0 g of **9b** as an orange solid. ^{1}H NMR (DMSO-d_6) δ = 8.27 (brs, 1 H, NH), 7.74 - 7.73 (m, 1H, Ph), 7.34 - 7.32 (m, 1H, Ph), 7.28 - 7.26 (m, 2H, Ph), 5.89 (d, *J*=7.6 Hz, 1H, OH), 5.03 (d, *J*=4.8 Hz, 1H, H-3), 4.97 (ddd, *J*=7.5, 4.9, 2.5 Hz, 1H, H-4), 4.55 - 4.53 (m, 1H, Cp), 4.41 - 4.40 (m, 1H, Cp), 4.38 - 4.37 (m, 1H, Cp), 4.35 - 4.34 (m, 1H, Cp), 4.16 (s, 5H, Cp); ^{13}C{^{1}H} NMR (DMSO-d_6) δ = 170.1 (C-2), 137.4 (C_{Ph}), 135.3 (C_{Ph}), 130.3 (CH_{Ph}), 127.0 (CH_{Ph}), 126.5 (CH_{Ph}), 125.7 (CH_{Ph}), 86.2 (Cp_{ipso}), 79.7 (C-4), 70.9 (Cp), 69.2 (Cp), 68.3 (Cp), 68.2 (Cp), 67.9 (Cp), 55.4 (C-3); Elemental analysis for $C_{19}H_{17}FeNO_2$ Calculated C-65.73, H-4.94, N-4.03 found C-65.69, H-4.93, N-3.95. Both enantiomers of **9b** were separated using preparative HPLC on a chiral semi-preparative column (Cellulose-1 10 × 250 mm) using n-hexane/IPA (60:40) as the eluent at a flow rate of 10 mL/min. (*3S,4R*)-**9b** eluted at τ=3.45 min and (*3R,4S*)-**9b** at τ=4.84 min. Both isomers had the same NMR spectra as the racemic mixture of **9b**. (*3S,4R*)-**9b**: $[\alpha]_D^{20}$= -247° ($CHCl_3$), HPLC, Lux Cellulose-1, 4.6 mm × 250 mm, hexane/IPA (50:50), 1 ml/min, 324 nm, optical purity 100% of (-)-isomer, τ=7.18 min. (*3R,4S*)-**9b**: $[\alpha]_D^{20}$ = +239° ($CHCl_3$), HPLC, Lux Cellulose-1, 4.6 mm × 250 mm, hexane/IPA (50:50), 1 ml/min, 324 nm, optical purity 97.4 % of (+)-isomer, τ=9.02 min).

General procedure C - *O*-triethylsilylation of azetidinones 10a-d

***cis*-4-ferrocenyl-3-(triethylsilyloxy)azetidin-2-one** (**10a**)

1.53 g (1.70 mL, 10.1 mmol) of TESCl was added to a solution of the crude **9a** (2.50 g, 6.49 mmol) in 80 mL of anhydrous pyridine, and the resulting solution was stirred at RT for 50 min. Then 200 mL of water was added and the product was extracted with ethyl acetate. The organic phase was washed with water, brine and dried. Chromatography on silica gel (250 mL) using n-hexane/ethyl acetate (4:1) as the eluent gave **10a** in 80% yield (2.84 g) as yellow crystals. ^{1}H NMR (DMSO-d_6) δ = 8.41 (brs, 1H, NH), 4.82 (dd, *J*=4.4, 2.5 Hz, 1H, H-4), 4.48 (d, *J*=4.6 Hz, 1H, H-3), 4.19 (s, 5H, Cp), 4.16 - 4.14 (m, 2H, Cp), 4.14 (brs, 1H, Cp), 4.09 (s, 1H, Cp), 0.78 (t, *J*=8.0 Hz, 9H, TES), 0.47 - 0.34 (m, 6H, TES); ^{13}C{^{1}H} NMR (DMSO-d_6) δ = 168.8 (C-2), 84.5 (Cp_{ipso}), 77.6 (C-4), 68.2 (Cp), 68.1 (Cp), 67.5 (Cp), 67.3 (Cp), 66.1 (Cp), 54.9 (C-3), 6.2 (TES), 4.0 (TES); Elemental analysis for $C_{19}H_{27}FeNO_2Si$ Calculated C-59.22, H-7.06, N-3.63 found C-61.08, H-7.08, N-3.50. Both enantiomers of **10a** were separated using preparative HPLC on a chiral preparative column (Cellulose-2 21.2 × 150 mm) using acetonitrile/water (9:1) as the eluent at a flow rate of 25 mL/min. (*3S,4R*)-**10a** (1.25 g) eluted at τ=4.08 min and (*3R,4S*)-**10a** (1.28 g) at τ=5.22 min. Both compounds had the same NMR spectra as the racemic mixture of **10a**. (*3S,4R*)-**10a**: $[\alpha]_D^{20}$= +275° ($CHCl_3$); HPLC, Lux Cellulose-2, 4.6 mm × 150 mm, n-hexane/IPA (70:30), 1 mL/min, 222 nm, optical purity 100% of (+)-isomer, τ=9.00 min. (*3R,4S*)-**10a**: $[\alpha]_D^{20}$= -267° ($CHCl_3$); HPLC, Lux Cellulose-2, 4.6 mm × 150 mm, n-hexane/IPA (70:30), 1 mL/min, 222 nm, optical purity 98.1% of (-)-isomer, τ=15.93 min.

General procedure D – *N*-benzoylation of azetidinin-2-ones 10a-d to 11a-d

(*3S,4R*)-1-benzoyl-4-ferrocenyl-3-(triethysilyloxy)azetidin-2-one ((*3S,4R*)-**11a**): 302 µL (366 mg, 2.60 mmol) of freshly distilled benzoyl chloride was added to a solution of 500 mg (1.30 mmol) of (*3S,4R*)-**10a**, 62 mg (0.51 mmol) of DMAP and 545 µL (396 mg, 3.91 mmol) of triethylamine in 9 mL of DCM, and the resulting solution was stirred at RT. After 2 h, the solvents were evaporated and the pure product was isolated using column chromatography on silica gel 200 mL with n-hexane/ethyl acetate (4:1) as the eluent. The pure product was isolated as an orange solid in 93% yield (591 mg). This compound is not very stable in solid state and in solution and was immediately used in the next step. Due to low stability it was not possible to obtain good elemental analysis and high quality NMR spectra. This compound was used in the next step immediately.^{1}H NMR ($CDCl_3$) δ = 8.01 (d, *J*=7.4 Hz, 2H, Ph), 7.61 (t, *J*=7.5 Hz, 1H, Ph), 7.49 (t, *J*=7.7 Hz, 2H, Ph), 5.33 (d, *J*=6.4 Hz, 1H, H-4), 5.04 (d, *J*=6.4 Hz, 1H, H-3), 4.30-4.29 (m, 2H, Cp), 4.21-4.19 (m, 7H, Cp), 0.94 (t, *J*=8.0 Hz, 9H, TES), 0.66-0.61 (m, 6H, TES); ^{13}C{^{1}H} NMR ($CDCl_3$) δ = 166.6 (COPh), 166.1 (C-2), 133.4 (CH_{Ph}), 132.5(C_{Ph}), 130.2 (CH_{Ph}), 128.1 (CH_{Ph}), 82.6 (Cp_{ipso}), 76.2 (C-4), 69.0 (Cp), 68.2 (Cp), 68.0 (Cp), 67.8 (Cp), 67.6 (Cp), 57.3 (C-3), 6.5 (TES), 4.6 (TES); $[\alpha]_D^{20}$= -173.4° ($CHCl_3$).

General procedure E – Synthesis of ferrocene-substituted paclitaxels

3'-dephenyl-3'-ferrocenyl-2',7-O-bis(triethylsilyl)paclitaxel (**12a**): A solution of 1.35 mL of LiHMDS (1M in THF, 1.35 mmol) was added to a solution of 450 mg (0.92 mmol) of (*3R,4S*)-1-benzoyl-4-ferrocenyl-3-(triethylililoxy)azetidin-2-one (*3R,4S*)-**11a** and 430 mg (0.61 mmol) of 7-triethylsilylbaccatin III **4** in 14.6 mL of anhydrous tetrahydrofurane at -40 °C and the resulting solution was stirred at this temperature for 40 min. After quenching of the reaction by addition of 50 mL of saturated ammonium chloride, the product was extracted with ethyl acetate. Chromatography on silica gel using n-hexane/ethyl acetate (3:1) as eluent gave 591 mg (81%) of the desired product as a yellow solid. ^{1}H NMR (DMSO-d_6) δ = 8.53 (d, *J*=9.8 Hz, 1H, NH), 8.05 (d, *J*=7.4 Hz, 2H, Ph), 7.94 (d, *J*=7.0 Hz, 2H, Ph), 7.70 (t, *J*=7.4 Hz, 1H, Ph), 7.58-7.51 (m, 5H, Ph), 6.29 (s, 1H, H-10), 6.01 (t, *J*=8.8 Hz, 1H, H-13), 5.46 (d, *J*=7.1 H, 1H, H-2), 5.33 (t, *J*=8.1 Hz, 1H, H-3'), 4.94 (d, *J*=9.6 Hz, 1H, H-5), 4.78 (s, 1H, 1-OH), 4.70 (s, 1H, Cp), 4.39 (dd, *J*=10.3, 6.8 Hz, 1H, H-7), 4.28 (d, *J*=6.7 Hz, 1H, H-2'), 4.24 (s, 1H, Cp), 4.17 (s, 1H, Cp), 4.10 (s, 6H, Cp), 4.07 (d, *J*=8.3 Hz, 1H, H-20), 4.03 (d, *J*=8.2 Hz, 1H, H-20), 3.66 (d, *J*=7.1 Hz, 1H, H-3), 2.49-2.45 (m, 1H, H-6), 2.26 (s, 3H, 4-OCOCH_3), 2.15 (dd, *J*=15.6, 9.2 Hz, 1H H-14), 2.10 (s, 3H, 10-OCOCH_3), 2.04 (dd, *J*=15.3, 9.2 Hz, 1H, H-14), 1.89 (s, 3H, H-18), 1.66 (brt, *J*=12.2 Hz, 1H, H-6), 1.55 (s, 3H, H-19), 1.07 (s, 6H, H-16 and H-17), 0.86 (t, *J*=7.9 Hz, 9H, TES), 0.81 (t, *J*=7.9 Hz, 9H, TES), 0.56-0.45 (m, 12H, TES); ^{13}C{^{1}H} NMR (DMSO-d_6) δ = 201.3 (C-9), 171.9 (C-1'), 169.8 (4-O<u>C</u>OCH$_3$), 168.8 (10-O<u>C</u>OCH$_3$), 166.6 (CONH), 165.1 (2-OCOPh), 139.0 (C-12), 135.2 (C_{Ph}), 133.5 (C-11), 133.3 (CH_{Ph}), 131.0 (CH_{Ph}), 129.9 (C_{Ph}), 129.6 (CH_{Ph}), 128.5 (CH_{Ph}), 128.1 (CH_{Ph}), 127.4 (CH_{Ph}), 86.6 (Cp_{ipso}), 83.1 (C-5), 79.8 (C-4), 76.7 (C-1), 75.6 (C-2'), 75.3 (C-20), 74.6 (C-10), 74.3 (C-2), 71.9 (C-7), 70.1 (C-13), 68.3 (Cp), 67.8 (Cp), 67.6 (Cp), 67.2 (2xCp), 57.6 (C-8), 52.1 (C-3'), 45.9 (C-3), 42.9 (C-15), 36.6 (C-6), 34.9 (C-14), 26.2 (C-16 or C-17), 22.8 (4-OCO<u>C</u>H$_3$), 21.0 (C-16 or C-17), 20.4 (10-OCO<u>C</u>H$_3$), 13.8 (C-18), 9.7 (C-19), 6.4 (TES), 4.7 (TES), 4.1 (TES); MS (ESI) for $C_{63}H_{83}FeNO_{14}Si_2$ calculated 1189.5 found 1189.4 (M^+); $[\alpha]_D^{20}$= -13.7° ($CHCl_3$).

General procedure F – Desilylation of *O*-2',7-bis(triethylsilyl)paclitaxels

***N*-debenzoyl-*N*-(2-ferrocenylbenzoyl)paclitaxel** (**6b**): 3.1 mL HF·PyH was added to a solution of 340 mg (0.268 mmol) of **5b** in a mixture of 12.5mL of MeCN and 23 mL pyridine (Teflon-made flask was used). The resulting solution was stirred at RT overnight (20h) and 50 mL of ethyl acetate and 200 mL of sodium bicarbonate were added. Crude product was extracted with ethyl acetate. Chromatography on silica using gradient of MeOH in DCM as eluent starting from 0% to 5% of MeOH gave pure **6b** in 95 % yield (264 mg of a pale yellow solid). ^{1}H NMR (DMSO-d_6) δ = 8.90 (d, *J*=8.9 Hz, 1H, NH), 7.97 (d, *J*=7.3 Hz, 2H, Ph), 7.80 (d, *J*=7.6 Hz, 1H, Ph), 7.71 (t, *J*=7.4 Hz, 1H, Ph), 7.62 (t, *J*=7.7 Hz, 2H, Ph), 7.42-7.38 (m, 3H, Ph), 7.35 (d, *J*=7.3 Hz, 2H, Ph), 7.26 (t, *J*=7.6 Hz, 1H, Ph), 7.23 (t, *J*=7.3 Hz, 1H, Ph), 7.18 (d, *J*=6.8 Hz, 1H, Ph), 6.32 (s, 1H, H-10), 6.10 (d, *J*=7.4 Hz, 1H, 2'-OH), 5.91 (t, *J*=8.8 Hz, 1H, H-13), 5.44 (d, *J*=7.2 Hz, 1H, H-2), 5.31 (t, *J*=8.2 Hz, 1H, H-3'), 4.91-4.89 (m, 2H, H-5 and 7-OH), 4.71 (s, 1H, 1-OH), 4.61 (brs, 1H, Cp), 4.50-4.47 (m, 2H, H-2' and Cp), 4.17 (brs, 1H, Cp), 4.14 (brs, 1H, Cp), 4.12-4.08 (m, 1H, H-7), 4.04-4.00 (m, 7H, Cp and H-20), 3.62 (d, J=7.1 Hz, 1H, H-3), 2.35-2.29 (m, 1H, H-6), 2.22 (s, 3H, 4-OCOCH$_3$), 2.12 (s, 3H, 10-OCOCH$_3$), 1.91 (dd, *J*=15.2, 9.2 Hz, 1H, H-14), 1.80 (s, 3H, H-18), 1.75 (dd, *J*=15.2, 9.1 Hz, 1H, H-14), 1.66-1.62 (m, 1H, H-6), 1.51 (s, 3H, H-19), 1.06 (s, 3H, H-16 or 17), 1.05 (s, 3H, H-16 or 17); ^{13}C{^{1}H} NMR (DMSO-d_6) δ = 202.3 (C-9), 172.7 (C-1'), 169.8 (4-O<u>C</u>OCH$_3$), 169.1 (CONH), 168.7 (10-O<u>C</u>OCH$_3$), 165.2 (2-O<u>C</u>OPh), 139.3 (C-12), 138.7 (C$_{Ph}$), 136.3 (C$_{Ph}$), 136.2 (C$_{Ph}$), 133.3 (C-11 and CH$_{Ph}$), 129.9 (CH$_{Ph}$), 129.5 (CH$_{Ph}$), 128.6 (CH$_{Ph}$), 128.2 (2× CH$_{Ph}$), 127.6 (CH$_{Ph}$), 127.4 (CH$_{Ph}$), 127.2 (CH$_{Ph}$), 125.3 (CH$_{P}$h), 83.6 (C-5), 80.2 (C-4), 76.7 (C-1), 75.3 (C-20), 74.7 (C-10), 74.5 (C-2), 73.8 (C-2'), 70.4 (C-7), 69.6 (C-13), 69.4 (Cp), 69.3 (Cp), 68.3 (Cp), 68.1 (2xCp), 57.4 (C-3'), 46.1 (C-3), 42.9 (C-15), 36.5 (C-6), 34.6 (C-14), 26.3 (C-16 or C-17), 22.4 (4-OCOCH$_3$), 21.2 (C-16 or C-17), 20.6 (10-OCOCH$_3$), 13.9 (C-18), 9.7 (C-19); MS (ESI) for $C_{57}H_{59}FeNO_{14}$ calculated 1037.3 found 1037.3 (M^+) 1060.3 ($M+Na)^+$; $[\alpha]_D^{20}$= -42.9° ($CHCl_3$).

Docking

The derivatives were docked to the crystal structure of tubulin with the PDB ID 1JFF[19a] Scigress v2.6[21] was used to prepare the crystal structure for docking, i.e. the hydrogen atoms were added, the co-crystallised ligands as well as crystallographic water molecules were removed. The Scigress software suite was also used to build the chemical structures, which were optimised using the MM2 force field[22] and the PM6 semi-empirical method[23]. The centre of the binding was defined in the tubulin structure as C13 of co-crystallised paclitaxel (x = 1.403, y = -16.979, z = 16.391) with a 10 Å radius. Fifty docking runs were allowed for each ligand with default search efficiency (100%). The basic amino acids lysine and arginine were defined as protonated. Furthermore, aspartic and glutamic acids were assumed to be deprotonated. The GoldScore (GS)[24] scoring function was implemented to validate the predicted binding modes and relative energies of the ligands using the GOLD v5.4.0 software suite.

Cytotoxicity

Solutions of all tested compounds were prepared freshly for every experiment and processed immediately. Stock solutions were prepared in DMSO and all compounds were added to cells to a final DMSO concentration of 0.2 % (v/v), while controls were incubated with 0.2 % DMSO alone. The chosen DMSO concentration was determined to be non-toxic to the cells.

Viability assay

The drug sensitivity of the cell lines was determined using the neutral red uptake assay.[25] Briefly, cells were seeded on 96-well plates at a density of 10,000/well and 24 h later were treated with control or test compound at a desired concentration. After 70 h of incubation, neutral red was added to the medium to a final concentration of 1 mM. After further 2 h of incubation, the cells were washed with PBS, dissolved in 200 µL solubilisation solution (1% acetic acid (v/v) in 50% ethanol (v/v)) and shaked for 10 min, until the neutral red was extracted from the cells. The absorbance was measured at 540 nm within EnVision Multilabel Plate Reader (PerkinElmer). The results were calculated as a percentage of controls and the IC_{50} values for each cell line and substance were calculated with the GraphPad Prism 5.02 software (GraphPad Inc.) using a four-parameter nonlinear logistic regression.

Tubulin polymerisation assay

The tubulin polymerisation rate was determined using a fluorescence-based tubulin polymerisation assay (Cytoskeleton, Inc., Cat. #BK011P) according to the manufacturer's instructions. The investigated compounds were tested over the concentrations range of 0.1–30 µM using freshly-prepared DMSO stock solutions and a final DMSO concentration of 1% was kept constant among all samples. Paclitaxel was used as a positive control of tubulin polymerisation and the results were compared to the solvent control (buffer + DMSO). The fluorescence was measured at 37 °C for 120 min at 355/40 nm excitation and 430/8 nm emission wavelengths using an EnVision Multilabel Plate Reader (Perkin Elmer).

Cell cycle analysis

Exponentially growing cells (100,000 cells/well seeded in 6-well plates 24 h before time 0) were treated with 10 nM of the test compound for 48 h. Cells were then harvested by trypsinisation, washed twice with ice-cold PBS and fixed in 70% ethanol. After storing the cells for at least 8 h at 4 °C, they were stained with propidium iodide staining solution (75 µM propidium iodide and 50 Kunitz units/mL of RNAse A in PBS) for 30 min at 37 °C. The samples were analysed on an LSRII (Becton Dickinson) flow cytometer and cell cycle phase distribution were determined with FlowJo 7.6.1 software (FlowJo, LLC) using a built-in cell cycle analysis module (Watson pragmatic algorithm).

ROS generation

The intracellular reactive oxygen species production was detected using dihydrorhodamine 123 as an oxidation-sensitive probe (DHR). DHR is a cell-permeable fluorogenic probe which is oxidized to fluorescent rhodamine 123 in the cells. In this study, exponentially growing cells (100,000 cells/well seeded in 6-well plates 48 h before time 0) were treated with 1 µM of the DHR for 4 h. During this period, the cells were treated with 1 µM of a test compound for a specific time prior to harvesting and washing with PBS. The samples were analysed with LSRII (Becton Dickinson) flow cytometer. ROS production was determined as a slope of the regression line of median DHR fluorescence intensity versus treatment time (i.e. DHR oxidation rate).

Acknowledgements

This work was financially supported by the National Science Centre Poland (NCN) based on the decision DEC-2012/05/B/ST5/00300. A.M. and S.P. also thanks for the National Science Centre Poland (NCN) for financial support,

(decision DEC-2012/04/A/ST5/00609), which enabled the X-ray structural analysis of the compounds.

Supporting information

CCDC 1543929-1543930, and 1544139-1544142 contains the supplementary crystallographic data for this paper. These data are provided free of charge by the Cambridge Crystallographic Data Centre.

Keywords: ferrocenyl taxanes • tubulin polymerisation • ROS generation • anticancer properties • ABCB1

[1] R. J. van Vuuren, M. H. Visagie, A. E. Theron and A. M. Joubert, *Cancer Chemother. Pharmacol.* **2015**, *76*, 1101-1112.

[2] B. A. Weaver, *Mol. Biol. Cell* **2014**, *25*, 2677-2681.

[3] a) D. G. I. Kingston, *J. Nat. Prod.* **2009**, *72*, 507-515; b) A. V. Singh, M. Bandi, N. Raje, P. Richardson, M. A. Palladino, D. Chauhan and K. C. Anderson, *Blood* **2011**, *117*, 5692-5700.

[4] E. Galletti, M. Magnani, M. L. Renzulli and M. Botta, *ChemMedChem* **2007**, *2*, 920-942.

[5] a) S. S. Braga and A. M. S. Silva, *Organometallics* **2013**, *32*, 5626-5639; b) G. Jaouen, A. Vessières and S. Top, *Chem. Soc. Rev.* **2015**, *44*, 8802-8817.

[6] a) A. Błauż, B. Rychlik, A. Makal, K. Szulc, P. Strzelczyk, G. Bujacz, J. Zakrzewski, K. Woźniak and D. Plażuk, *ChemPlusChem* **2016**, *81*, 1191-1201; b) J. D. J. Cázares-Marinero, S. Top, A. Vessières and G. Jaouen, *Dalton Trans.* **2014**, *43*, 817-830; c) E. Hillard, A. Vessières, F. Le Bideau, D. Plazuk, D. Spera, M. Huché and G. Jaouen, *ChemMedChem* **2006**, *1*, 551-559; d) J. L. Kedge, H. V. Nguyen, Z. Khan, L. Male, M. K. I. H. V. R. N. Hodges, S. L. Horswell, Y. Mehellou and J. H. R. Tucker, *Eur. J. Inorg. Chem.* **2017**, *2017*, 466-476; e) M. Librizzi, A. Longo, R. Chiarelli, J. Amin, J. Spencer and C. Luparello, *Chem. Res. Toxicol.* **2012**, *25*, 2608-2616; f) J. K. Muenzner, B. Biersack, A. Albrecht, T. Rehm, U. Lacher, W. Milius, A. Casini, J. J. Zhang, I. Ott, V. Brabec, O. Stuchlikova, I. C. Andronache, L. Kaps, D. Schuppan and R. Schobert, *Chem. Eur. J.* **2016**, *22*, 18953-18962; g) C. Ornelas, *New J. Chem.* **2011**, *35*, 1973-1985; h) D. Plazuk, B. Rychlik, A. Błauz and S. Domagała, *J. Organomet. Chem.* **2012**, *715*, 102-112; i) M. Beauperin, S. Top, M.-A. Richard, D. Plazuk, P. Pigeon, S. Toma, V. Polackova and G. Jaouen, *Dalton Trans.* **2016**, *45*, 13126-13134; j) D. Plażuk, S. Top, A. Vessieres, M.-A. Plamont, M. Huche, J. Zakrzewski, A. Makal, K. Woźniak and G. Jaouen, *Dalton Trans.* **2010**, *39*, 7444-7450; k) D. Plazuk, A. Wieczorek, A. Blauz and B. Rychlik, *MedChemComm* **2012**, *3*, 498-501; l) A. Wieczorek, A. Blauz, A. Makal, B. Rychlik and D. Plazuk, *Dalton Trans.* **2017,** 46, 10847 - 10858; m) J. Spencer, J. Amin, M. Wang, G. Packham, S. S. S. Alwi, G. J. Tizzard, S. J. Coles, R. M. Paranal, J. E. Bradner and T. D. Heightman, *ACS Med. Chem. Lett.* **2011**, *2*, 358-362.

[7] a) G. Mwande Maguene, J. B. Lekana-Douki, E. Mouray, T. Bousquet, P. Grellier, S. Pellegrini, F. S. Toure Ndouo, J. Lebibi and L. Pélinski, *Eur. J. Med. Chem.* **2014**, *90*, 519-525; b) C. Reiter, T. Fröhlich, M. Zeino, M. Marschall, H. Bahsi, M. Leidenberger, O. Friedrich, B. Kappes, F. Hampel, T. Efferth and S. B. Tsogoeva, *Eur. J. Med. Chem.* **2015**, *97*, 164-172; c) P. F. Salas, C. Herrmann, J. F. Cawthray, C. Nimphius, A. Kenkel, J. Chen, C. De Kock, P. J. Smith, B. O. Patrick, M. J. Adam and C. Orvig, *J. Med. Chem.* **2013**, *56*, 1596-1613; d) S. Vandekerckhove and M. D'Hooghe, *Bioorganic and Medicinal Chemistry* **2015**, *23*, 5098-5119; e) W. A. Wani, E. Jameel, U. Baig, S. Mumtazuddin and L. T. Hun, *Eur. J. Med. Chem.* **2015**, *101*, 534-551; f) A. Patti, S. Pedotti, T. Grassi, A. Idolo, M. Guido and A. De Donno, *J. Organomet. Chem.* **2012**, *716*, 216-221; g) D. Dive and C. Biot, *ChemMedChem* **2008**, *3*, 383-391.

[8] a) M. Görmen, M. S.-I. Veitía, F. Trigui, M. El Arbi and C. Ferroud, *J. Organomet. Chem.* **2015**, *794*, 274-281; b) B. Long, C. He, Y. Yang and J. Xiang, *Eur. J. Med. Chem.* **2010**, *45*, 1181-1188; c) G. M. Maguene, J. Jakhlal, M. Ladyman, A. Vallin, D. A. Ralambomanana, T. Bousquet, J. Maugein, J. Lebibi and L. Pélinski, *Eur. J. Med. Chem.* **2011**, *46*, 31-38; d) E. Rami Reddy, R. Trivedi, L. Giribabu, B. Sridhar, K. Pranay Kumar, M. Srinivasa Rao and A. V. S. Sarma, *Eur. J. Inorg. Chem.* **2013**, 5311-5319.

[9] B. Kater, A. Hunold, H.-G. Schmalz, L. Kater, B. Bonitzki, P. Jesse and A. Prokop, *J. Cancer Res. Clin. Oncol.* **2011**, *137*, 639-649.

[10] C. Lu, J. M. Heldt, M. Guille-Collignon, F. Lemaître, G. Jaouen, A. Vessières and C. Amatore, *ChemMedChem* **2014**, *9*, 1286-1293.

[11] F. Dubar, J. Khalife, J. Brocard, D. Dive and C. Biot, *Molecules* **2008**, *13*, 2900-2907.

[12] A. Wieczorek, A. Błauż, J. Zakrzewski, B. Rychlik and D. Plażuk, *ACS Med. Chem. Lett.* **2016**, *7*, 612-617.

[13] a) X. Peng and V. Gandhi, *Ther. Deliv.* **2012**, *3*, 823-833; b) M. Schikora, A. Reznikov, L. Chaykovskaya, O. Sachinska, L. Polyakova and A. Mokhir, *Bioorg. Med. Chem. Lett.* **2015**, *25*, 3447-3450.

[14] A. Wieczorek, A. Błauż, A. Żal, H. J. Arabshahi, J. Reynisson, C. G. Hartinger, B. Rychlik and D. Plażuk, *Chem. Eur. J.* **2016**, *22*, 11413-11421.

[15] A. Błauż and B. Rychlik, *J. Pharmacol. Toxicol. Methods* **2017**, *84*, 57-65.

[16] a) P. Wils, V. Phung-Ba, A. Warnery, D. Lechardeur, S. Raeissi, I. J. Hidalgo and D. Scherman, *Biochem. Pharmacol.* **1994**, *48*, 1528-1530; b) E. Mechetner, A. Kyshtoobayeva, S. Zonis, H. Kim, R. Stroup, R. Garcia, R. J. Parker and J. P. Fruehauf, *Clin. Cancer Res.* **1998**, *4*, 389-398.

[17] K. O. Hamilton, G. Backstrom, M. A. Yazdanian and K. L. Audus, *J. Pharm. Sci.* **2001**, *90*, 647-658.

[18] a) J. Alexandre, F. Batteux, C. Nicco, C. Chereau, A. Laurent, L. Guillevin, B. Weill and F. Goldwasser, *Int. J. Cancer* **2006**, *119*, 41-48; b) J. Alexandre, Y. Hu, W. Lu, H. Pelicano and P. Huang, *Cancer Res.* **2007**, *67*, 3512-3517; c) B. Ramanathan, K.-Y. Jan, C.-H. Chen, T.-C. Hour, H.-J. Yu and Y.-S. Pu, *Cancer Res.* **2005**, *65*, 8455.

[19] a) J. Löwe, H. Li, K. Downing and E. Nogales, *J. Mol. Biol.* **2001**, *313*, 1045-1057; b) J. P. Snyder, J. H. Nettles, B. Cornett, K. H. Downing and E. Nogales, *Proc. Natl. Acad. Sci. U.S.A.* **2001**, *98*, 5312-5316.

[20] P. Vu; R. A. Holton U.S. Patent No 7,550,608, 2009

[21] Scigress v2.6 Fujitsu

[22] N. L. Allinger, *J. Am. Chem. Soc.* **1977**, *99*, 8127-8134.

[23] J. J. Stewart, *J. Mol. Model.* **2007**, *13*, 1173-1213.

[24] G. Jones, P. Willet, R. C. Glen, A. R. Leach and R. Taylor, *J.Mol.Biol.* **1997**, *267*, 727-748.

[25] G. Repetto, A. Del Peso and J. L. Zurita, *Nat. Protoc.* **2008**, *3*, 1125-1131.

10.1002/cmdc.201700576

WILEY-VCH

Entry for the Table of Contents

FULL PAPER

Two series of ferrocenyl-decorated paclitaxels were synthesised and their anticancer properties were studied. The cytotoxic activity of these compounds strongly dependent on the position of the ferrocenyl group, with the *N*-benzoyl substituted compounds **6a-d** being the most active derivatives. The substitution of a 3'-phenyl group with a ferrocenyl moiety (**13b** and **13c**) leads to compounds able to overcome multidrug resistance as they are virtually unrecognized by ABCB1.

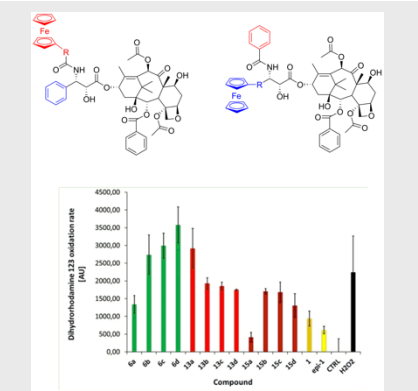

Damian Plażuk, Anna Wieczorek, Wojciech M. Ciszewski, Karolina Kowalczyk, Andrzej Błauż, Sylwia Pawlędzio, Anna Makal, Chatchakorn Eurtivong, Homayon J. Arabshahi, Jóhannes Reynisson, Christian G. Hartinger, Błażej Rychlik*

Page No. – Page No.

Synthesis and Evaluation of *In Vitro* Biological Properties of Ferrocenyl Side-Chain-Decorated Paclitaxel